frontiers in Materials

ORIGINAL RESEARCH
published: 08 February 2021
doi: 10.3389/fmats.2020.622669

Rational Design and Fabrication of Biomimetic Hierarchical Scaffolds With Bone-Matchable Strength for Bone Regeneration

Ruixian Lian[1], Peng Xie[1], Lan Xiao[2,3], Zoya Iqbal[1], Shihao Zhang[4], Joachim Kohn[5], Xue Qu[1], Changsheng Liu[1] and Yulin Li[1]**

[1]*The State Key Laboratory of Bioreactor Engineering and Key Laboratory for Ultrafine Materials of Ministry of Education, Key Laboratory for Ultrafine Materials of Ministry of Education, Engineering Research Centre for Biomedical Materials of Ministry of Education, East China University of Science and Technology, Shanghai, China,* [2]*Institute of Health and Biomedical Innovation, Queensland University of Technology, Brisbane, QLD, Australia,* [3]*The Australia-China Centre for Tissue Engineering and Regenerative Medicine (ACCTERM), Brisbane, QLD, Australia,* [4]*New Organic Chemical Materials Hubei Collaborative Innovation Center, Key Laboratory of Organic Functional Molecular Synthesis and Application of Ministry of Education, College of Chemistry and Chemical Engineering, Hubei University, Wuhan, China,* [5]*Department of Chemistry and Chemical Biology, New Jersey Center for Biomaterials, Piscataway, NJ, United States*

OPEN ACCESS

Edited by:
Iman Roohani, University of New South Wales, Australia

Reviewed by:
Yifan Ma, The Ohio State University, United States
Jiao Jiao Li, University of Technology Sydney, Australia

***Correspondence:**
Yulin Li
yulinli@ecust.edu.cn
Joachim Kohn
Kohn@dls.rutgers.edu

Specialty section:
This article was submitted to Biomaterials, a section of the journal Frontiers in Materials

Received: *29 October 2020*
Accepted: *23 December 2020*
Published: *08 February 2021*

Citation:
Lian R, Xie P, Xiao L, Iqbal Z, Zhang S, Kohn J, Qu X, Liu C and Li Y (2021) Rational Design and Fabrication of Biomimetic Hierarchical Scaffolds With Bone-Matchable Strength for Bone Regeneration. Front. Mater. 7:622669. doi: 10.3389/fmats.2020.622669

The development of scaffolds with bone-mimicking compositions, hierarchical structure, and bone-matchable mechanical properties may offer a novel route for the achievement of effective bone regeneration. Although bioactive glasses have been widely utilized for bone regeneration at the clinical level, their brittleness and uncontrolled pore structure limit further applications. Herein, this study aims to develop a kind of bioactive scaffold with a macroporous/microporous/mesoporous structure *via* impregnating a sponge template with mesoporous bioactive glass (MBG) sol, followed by sponge template removal. In order to improve the mechanical properties and stability of the MBG scaffolds, desaminotyrosyl ethyl tyrosine polycarbonates (PDTEC), a biodegradable polymer which does not induce acid side-effects caused by conventional polylactide, was selected to decorate the resulting hierarchical scaffolds through a surface coating approach. The PDTEC functionalization endowed the scaffolds with improved mechanical strength matching the bearable range of trabecular bone (2–12 MPa). Meanwhile, the relative neutral pH value was maintained during their degradation process. *In vitro* studies demonstrated that the PDTEC accelerated the biomineralization of the scaffolds, and promoted the attachment and proliferation, holding high promise for bone regeneration.

Keywords: bioactive glass, polymer coating, sol–gel method, bone mimicking hierarchical scaffolds, biomineralization, bone regeneration

INTRODUCTION

Designing novel biomaterials represents an essential strategy in bone tissue engineering. Bone fractures, bone tumors, osteoporosis, and other orthopedic diseases caused by natural disasters, industrial pollution, and the aging population pose a serious threat to human health (Bosetti and Cannas, 2005; Zhou et al., 2017). The treatment of orthopedic diseases includes the introduction of

autologous bone, allogeneic bone, and the employment of synthetic implants with specific structures and properties (Yang et al., 2015). These offer the insight that the development of synthetic scaffolds with compositional and structural features mimicking natural bone tissues may enable the production of artificial bone implants with both high biosafety and bioactivity.

It is known that bone is a kind of multi-level structured tissue, which owns cancellous and cortical bone parts at the macrostructure level, trabeculae parts at the microstructure level, lamellae units at the sub-microstructure level, and fibrillar collagen and embedded minerals at the sub-nanostructure level (Baino et al., 2016; Tang et al., 2016; Schumacher et al., 2017). The hierarchical architecture of natural bone provides the proper microenvironment for the maintenance of their metabolically activity, such as promoting nutrient exchange and waste removal processes, offering sufficient space for cell movements, proliferation, differentiation, promoting bone formation, and improving the functional activities of the tissue (García et al., 2011; Baino et al., 2016; Xie et al., 2019). Generally, the nanosized structures (2–50 nm) afford high surface area and specific surfaces/interfaces for the administration of bioactive growth factors to improve bone regeneration by upregulating the FAK/MAPK and ILK/β-catenin signaling pathways as shown in our previous studies (Tang et al., 2014; Vallet-Reg, 2016; Duan et al., 2017). Microsized porous structures (~10 μm) are conducive to protein adsorption, cell adhesion biomineralization, the osteogenic differentiation of stem cells, and the integration of materials and bones (Lin et al., 2015; Tang et al., 2016). The macropores (100–500 μm) allow for the promotion of vascularization, and the ingrowth of new bone and tissue (Baino et al., 2016; Zhou et al., 2016; Du et al., 2018).

Among inorganic materials, the special composition and structure of bioactive glasses make them widely applicable for bone regeneration (Aamer et al., 2009; Wu et al., 2010). A mesoporous bioactive glass scaffold (MBG, $CaO–SiO_2–P_2O_5$ system) is a kind of mesoporous biodegradable bone repair scaffold with a rich pore structure, due to its huge specific surface area, an ordered pore structure, narrow pore size distribution, and size adjustable, etc. MBG can release certain amounts of ions through the degradation process, which activate the adhesion, proliferation, and differentiation of cells with specific functions such as increasing the ligand binding affinity of a certain protein, and the effect of promoting apatite mineralization (Wu et al., 2011; Tang et al., 2016; Zeng et al., 2017). In order to improve the osteogenic activity of the material, different types of cells and growth factors have been loaded onto the biodegradable scaffold and transplanted to the bone defect site to stimulate bone regeneration and vascular regeneration (Wu et al., 2013; Cai et al., 2018). With the above advantages, mesoporous bioactive glass is widely used as a bone repair material. Therefore, researchers used different manufacturing methods to obtain mesoporous bioactive glass scaffolds. Xie et al. firstly prepared bioactive glass rods of different sizes, and then used the sol-gel method to obtain porous MBG scaffolds (Xie et al., 2019). Duan et al. successfully prepared 3D layered macro/nanoporous scaffolds through the sol-gel and multi-template methods (Duan et al., 2017). However, these scaffolds when prepared based on bioactive glass have low mechanical strength and are therefore difficult to use consistently in the bone regeneration field. In order to improve the mechanical strength of the scaffolds, there are strategies that combine tricalcium silicate and other silicate particles with bioactive glass through 3D printing and solidification (Pei et al., 2016), as well as through polymer coating methods (e.g., poly (glycerol sebacate) coating) to improve the mechanical strength of the base scaffold (Lin et al., 2015). These scaffolds may have some uncontrollable external degradation factors in the complex environment of the human body. Herein, we chose a degradable coating with the clinical application to enhance the porous bioactive glass scaffold.

Poly(desaminotyrosyl-tyrosine carbonate) (PDTEC) is a biodegradable tyrosine-derived polymer with good biocompatibility used in biomedical devices at the clinical level. It has been reported that conventional polylactide-based materials would not result in acid-induced inflammatory side-effects and thereby benefit tissue regeneration. Moreover, PDTEC can release small molecules of tyrosine to aid in metabolism, growth, and the development of cells; meanwhile, the surface exposed carboxylate groups and carboxylic groups could attract calcium ions, exhibiting bone apposition when in contact with bone tissue *in vivo* (Chauvel-Lebret, 1999; Tangpasuthadol et al., 2000a; Tangpasuthadol et al., 2000b; Kim et al., 2010; Fukushima, 2016).

Herein, we propose to develop a bioactive scaffold with a macroporous/microporous/mesoporous structure by impregnating the sponge template with mesoporous bioactive glass (MBG) sol and then removing the organic template to get a hierarchically-structured MBG scaffold (**Scheme 1**). Meanwhile, to improve the mechanical properties of the scaffold, we chose to add a biodegradable layer of Poly(desaminotyrosyl-tyrosine carbonate) (PDTEC) onto the scaffold (Kaushik et al., 2012; Goyal et al., 2017). The PDTEC-decorated scaffolds showed not only a mechanical matchable quality with trabecular bone (2–12 MPa), but also benefit the biomineralization process for promoting cell attachment and proliferation, promising a high potential in bone regeneration application.

MATERIALS AND METHODS

Chemical Reagents

Poly(desaminotyrosyl-tyrosine carbonate) (PDTEC) was kindly donated by Joachim Kohn (Rutgers, The State University of New Jersey, the New Jersey Center for Biomaterials). Anhydrous ethanol, tetraethyl orthosilicate, triethyl phosphate, dimethyl sulfoxide, hydrochloric acid, dichloromethane, and calcium dinitrate tetrahydrate were acquired from the Shanghai Macklin Biochemical Technology Co., Ltd (Shanghai, China). Pluronic F-127, methylcellulose, and 3-(4,5-dimethylthiazol-2-yl)-2,5-diphenyltetrazolium bromide (MTT) were acquired from Sigma-Aldrich (CA, United States).

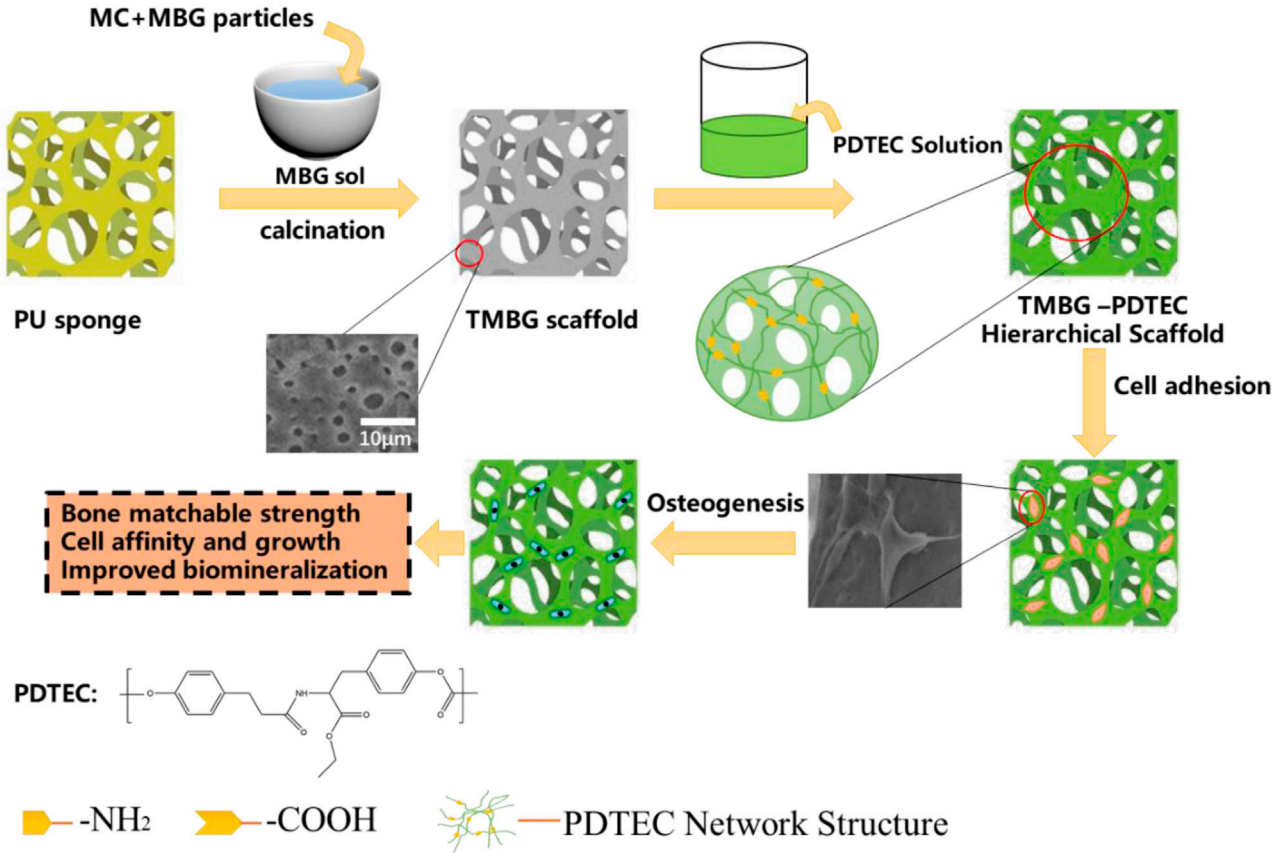

SCHEME 1 | Schematic illustration for the formation of a PDTEC-decorated MBG scaffold with a bone-mimicking macro/micro/meso-porous hierarchical structure and bone-matchable mechanical properties.

Fabrication of Triple Structure Mesoporous Bioactive Glass (TMBG) and TMBG-PDTEC Composite Scaffolds

TMBG and TMBG-PDTEC scaffolds were fabricated by a modified sol-gel and a polyurethane (PU) sponge template process was prepared according to a previously reported work with a minor modification (Xie et al., 2019). As in the typical fabrication procedure of TMBG, 4.0 g of F127 and 1 ml of HCl (1 M) were dissolved in 50 g of anhydrous ethanol and stirred at 40°C for 6 h, then 5.2 g of tetraethyl orthosilicate, 0.76 g of $Ca(NO_3)_2 \cdot 4H_2O$, 0.23 g of triethyl phosphate, and 1.0 ml of HCl (1 M) were dissolved in solution at 40°C for 1 day, followed by rotary evaporation for 30 min at 60°C to obtain an MBG sol with a viscosity of 5×10^4 Pa s. Then, the calculated MBG particles and methylcellulose (MC) were uniformly mixed with the sol, after the mixture was impregnated into the polyurethane (PU) sponge with the desired shape. The samples were placed in a dry oven at 60°C for 72 h and calcinated at 600°C for 6 h to remove all templates. After that we dissolved the PDTEC in dichloromethane to get the PDTEC solution. We chose a 16 wt% PDTEC solution and selected an 8 wt% PDTEC solution as a comparison, the prepared TMBG scaffolds were respectively soaked in the above-mentioned PDTEC solution for 1 min, then the composite scaffolds were dried in a vacuum for 2 days at 60°C (Zhu et al., 2018). The TMBG-PDTEC composite containing 8 wt% and 16 wt% PDTEC polymer were denoted as TMBG-PDTEC8 and TMBG-PDTEC16, respectively.

Characterization of the TMBG and TMBG-PDTEC Composite Scaffolds

The hierarchical porous morphology of TMBG and TMBG-PDTEC composite scaffolds were analyzed by scanning electron microscopy (SEM, S-3400, Hitachi, Japan) and transmission electron microscopy (HRTEM, JEM-2110F, JEOL, Ltd., Japan). The crystalline structures of TMBG and TMBG-PDTEC were characterized by an x-ray diffractometer (XRD, MAX2550VB, Japan). The scanning angle was from 10° to 80° with a scanning speed of 10°/min. The Fourier Transform Infrared spectra of TMBG and TMBG-PDTEC were performed on a Thermo FTIR instrument (FTIR; Nicolet 5700, United States). The scanned wavenumber range was from 4,000 to 500 cm^{-1}. A scaffold with a complete shape of Φ10 × 15 mm was chosen and placed in a vacuum drying oven at 60°C for 48 h to completely dry, and the porosity of the scaffold was tested according to Archimedes' principle:

$$P = \left(W_s - W_g\right)/\left(W_s - W_f\right) \times 100\%$$

where W_s is the weight of the scaffold saturated with water, W_g is the dry weight of the scaffold, and W_f is the weight of the scaffold immersed in water.

Each group of scaffolds was divided into five groups in parallel. The analysis of the compressive strength of the TMBG and TMBG-PDTEC scaffolds (Φ10 mm × 15 mm) was performed using a precision universal tester (universal testing machine, AG-2000A, Shimadzu, Japan) at ambient temperature with a crosshead speed of 1.0 mm/min.

In-vitro Degradation and Mineralization

The TMBG and TMBG-PDTEC scaffolds were immersed in the Tris–HCl buffer solution at a 1:200 proportion of scaffold weight (g) to solution volume (ml), and then placed in a constant temperature incubator shaker (37°C, 80 rpm). At each time point, the scaffolds were vacuum-dried and weighed, and the pH of the Tris-HCl solution was recorded. The *in vitro* biomineralization process of the scaffolds was examined through soaking them in simulated body fluid (SBF, pH 7.4) at a 1:200 proportion of scaffold weight (g) to solution volume (ml) in a constant temperature incubator shaker (37°C, 80 rpm). After this treatment process, the morphological condition of the mineralization was characterized by SEM, TEM, and x-ray diffraction (XRD) analysis.

Cell Viability, Proliferation, and Attachment

Rat bone marrow stromal cells (rBMSCs) were purchased from the Shanghai Institutes for Biological Sciences (SIBS, Shanghai, China). Primary rBMSCs expanded to passage 3 in growth media consisting of α-MEM with 10% (v/v) FBS and 1% (v/v) penicillin–streptomycin at 37°C in a humidified atmosphere of 5% CO_2 were used in all experiments. The cell morphology and spreading were visualized. The Φ10 mm × 2 mm TMBG and TMBG-PDTEC scaffolds were placed in a 48-well plate, inoculated with 4×10^3 rat bone marrow stromal cells per well and co-cultured for 24 h. After that, the cells were fixed on the scaffolds with glutaraldehyde solution (2.5% glutaraldehyde in PBS) for 15 min. Then, the samples were dehydrated in gradient alcohol for 5 min during each procedure, followed by immersion in isoamyl acetate for 20 min and vacuum-dried at 37°C for 4 h. The cell morphology was observed by SEM. The cell proliferation of the TMBG and TMBG-PDTEC scaffolds was examined by a Cell Counting Kit-8 assay (CCK-8, Dojindo, Kumamoto, Japan). rBMSCs were seeded on the Φ10 mm × 2 mm TMBG and TMBG-PDTEC scaffolds in a new 48-well plate at a density of 1×10^3 cells/well. After 1 day/4 days/7 days of co-cultivation, the cell culture medium was updated at the specified time point at the same time, 100 μL of cell culture medium from each well (in the 48-well plate) was transferred into a 96-well plate, with the addition of 10 μL of CCK-8 solution, then incubated at 37°C for 2 h. The absorbance at 450 nm was measured with a microplate reader (SPECTRAmax 384, Molecular Devices, United States). All measures were done in triplicate.

Statistics

Results were presented as mean ± standard deviation. All data were generated from at least three independent experiments ($n \geq 3$). A one-way ANOVA and Student–Newman–Keuls post hoc test were used to determine the level of significance, and a value of $p < 0.05$ was considered statistically significant.

RESULTS

Surface Morphology and Structural Analysis of TMBG and TMBG-PDTEC Scaffolds

The morphologies of the TMBG and TMBG-PDTEC scaffolds were investigated by SEM. As shown in **Figures 1A–C′**, the TMBG scaffolds consisted of a completely interconnected network structure with macropores (about 200–400 μm) and micro-sized pores (1–10 μm) uniformly distributed on their surface, which can facilitate cell migration, bone ingrowth, and the transport of nutrients and oxygen (Duan et al., 2017). The images of the scaffolds after being coated with two different loading contents of PDTEC are presented in **Figures 1B–C′**, indicating that the surface coating partially changed the microstructure of the scaffolds. The obtained scaffold was calculated to show a decreasing trend of porosity, which corresponded to the SEM image. The porosity of the TMBG scaffold was 87 ± 1.35%, while the porosity of the TMBG-PDTEC8 and TMBG-PDTEC16 scaffolds were 75 ± 1.56% and 61.5 ± 1.79%, respectively. This result showed that high-concentration surface coating may block some of the scaffold surface microporous structure. Interestingly, with a further increase of the PDTEC concentration (TMBG-PDTEC16), the coating network appeared on the scaffold surface, which may benefit bone ingrowth, the transport of nutrients and oxygen, and cell migration (Goyal et al., 2017). The changes in the thickness of the PDTEC coating can be observed from the cross-sectional images of the composite scaffolds with different amounts of PDTEC coating (**Figure 2**). The thickness of the TMBG-PDTEC8 scaffold coating was about 30 μm, and the thickness of the TMBG-PDTEC16 scaffold coating was about 50 μm. TEM observation indicated that mesopores existed among the scaffolds (Supplementary Figure 1). Therefore, scaffolds with a macro/micro/meso-porous hierarchical structure mimicking the architecture of natural bone have been successfully developed, which are potentially applicable for bone regeneration.

The compressive strength of the pristine TMBG and TMBG-PDTEC scaffolds were measured by compression testing. As shown in **Figure 3A**, the data clearly demonstrate that the compressive modulus of the TMBG scaffolds was 0.26 MPa. Although it was largely increased compared with traditional MBG scaffolds, it could not reach the minimum mechanical strength of trabecular bone (about 2 MPa). However, the compressive strength was significantly enhanced by increasing the PDTEC surface coating amount. The increase of PDTEC content from 8 to 16 wt% improved the compressive strength of the TMBG-PDTEC scaffolds from 0.26 to 2.76 MPa, which is similar to the matchable mechanical strength of trabecular bone

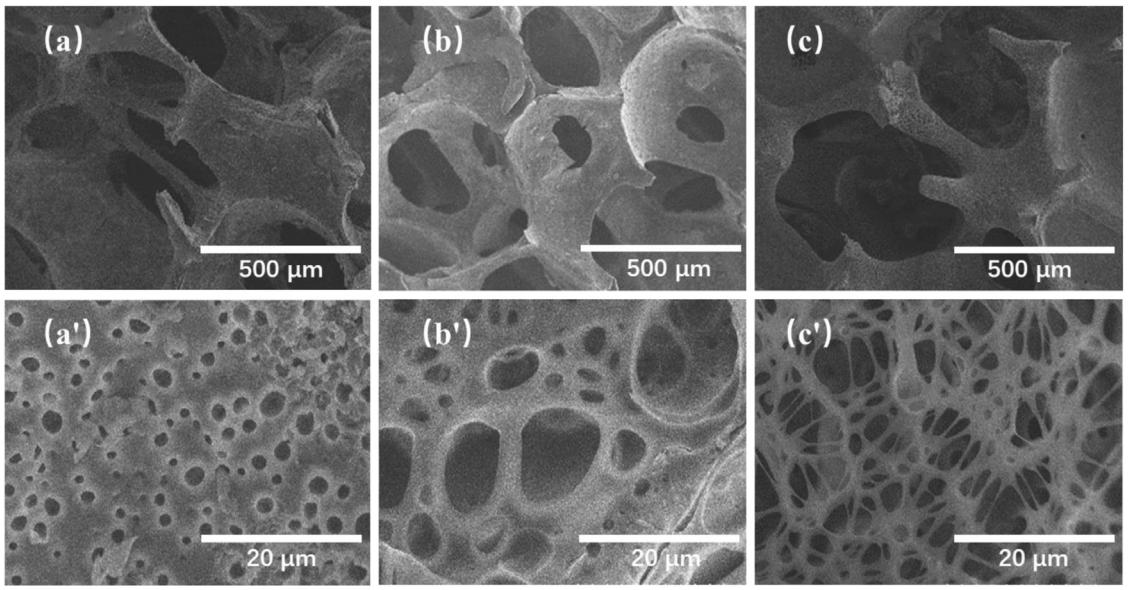

FIGURE 1 | SEM images of TMBG scaffolds before and after being coated with PDTEC: **(A**, **A′)** TMBG, **(B, B′)** TMBG-PDTEC8, and **(C, C′)** TMBG-PDTEC16 scaffolds.

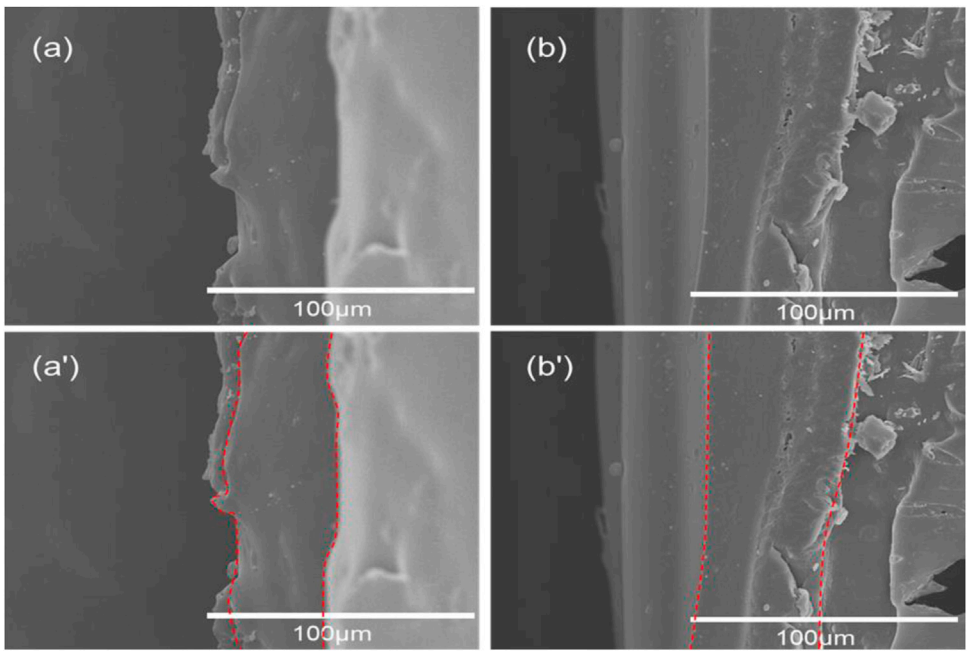

FIGURE 2 | Cross-sectional SEM images of composite scaffolds with different amounts of PDTEC coating: **(A, A′)** TMBG-PDTEC8 and **(B, B′)** TMBG-PDTEC16 scaffolds.

and would be more suitable for the application of bone regeneration.

The FTIR analysis was performed to confirm the successful incorporation of PDTEC into the TMBG scaffolds, and the results are displayed in **Figure 3B**. The FTIR spectrum of PDTEC showed typical absorption bands at 1512 and 1729 cm^{-1} which are characteristic of phenyl C=C stretching and carbonate C=O stretching, respectively. TMBG showed a spectra of peaks at 460 and 1079 cm^{-1} which could be assigned to the orthophosphate (PO_4^{3-}) group of TMBG (Yu and Kohn, 1999). The appearance of

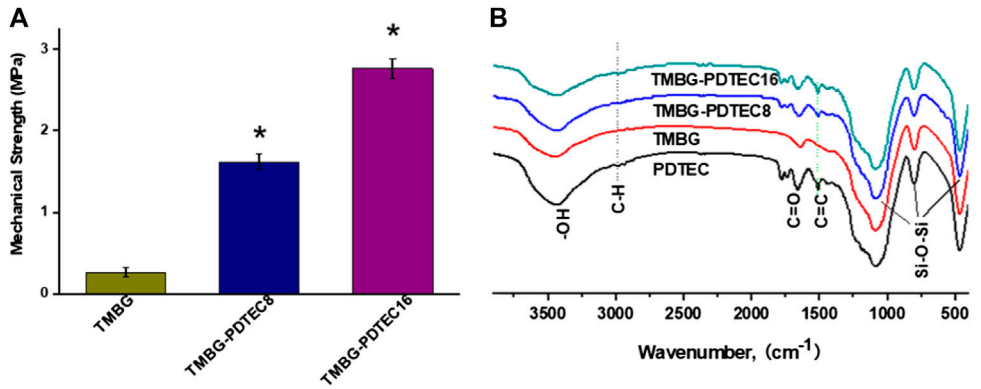

FIGURE 3 | Mechanical property and FTIR spectra of the scaffolds: **(A)** the compressive strength and **(B)** Fourier transform infrared (FTIR) spectroscopy patterns of prepared TMBG, TMBG-PDTEC8, and TMBG-PDTEC16 scaffolds. (*p < 0.05 compared to TMBG) (n = 5).

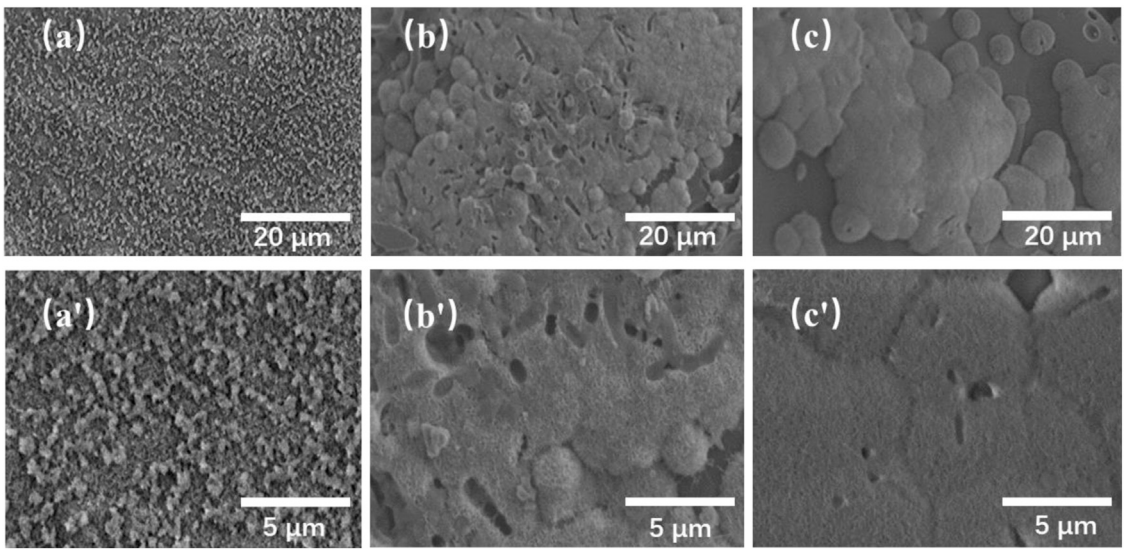

FIGURE 4 | SEM images of the TMBG **(A, A′)**, TMBG-PDTEC8 **(B, B′)**, and TMBG-PDTEC16 **(C, C′)** scaffolds after soaking in SBF for 3 days.

the bands for TMBG-PDTEC8 and TMBG-PDTEC16 revealed obvious PDTEC characteristic peaks of phenyl C=C stretching and carbonate C=O stretching, indicating the successful formation of PDTEC coating on the surface of the TMBG scaffolds (Kaushik et al., 2012; Yang et al., 2015).

In vitro Biomineralization and Biodegradability

The biomineralization properties of the TMBG and TMBG-PDTEC scaffolds upon immersion in simulated body fluid (SBF) were investigated. As shown in **Figure 4**, although all the scaffold surfaces presented mineralized depositions, the deposition amount significantly increased with polymer decoration. Furthermore, with the increasing amount of PDTEC, more and more apatite deposits were formed on the surface of the scaffolds, suggesting that adding the PDTEC significantly accelerated the biomineralization process (Marelli et al., 2011; Gu et al., 2017). To further analyze the phase composition of mineralization, the samples were tested by x-ray diffraction analysis (**Figure 5**). The main component of the scaffolds was disordered silica, and after SBF soaking, the diffraction peaks ($2\theta = 31^{\circ}$ and 45°) of hydroxyapatite in the XRD spectra of the TMBG-PDTEC scaffolds indicated that the PEDTC could promote biological mineralization upon soaking in SBF. This is probably because the hydrolysis of the pendent chains and the carbonate bonds of the PDTEC may be beneficial to the formation of the carboxyl groups, which have strong chelation to dissolved Ca ions to accelerate hydroxyapatite formation (Kaushik et al., 2012; Zhou et al., 2016; Souza et al., 2017).

Figure 6A shows the pH variation of the medium during degradation of the TMBG and TMBG-PDTEC scaffolds. The

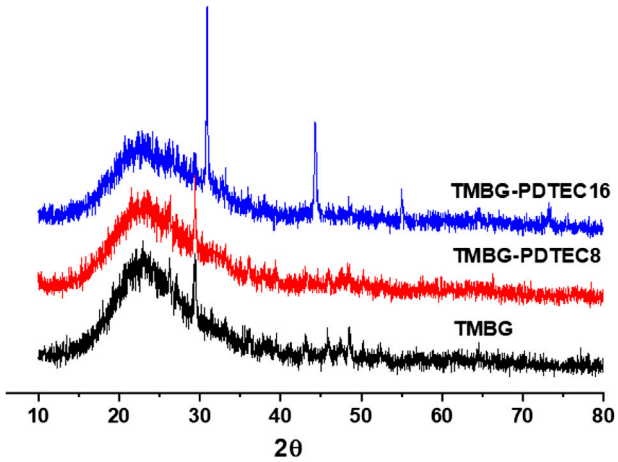

FIGURE 5 | X-ray diffraction (XRD) spectra of the scaffolds (TMBG, TMBG-PDTEC8, and TMBG-PDTEC16) after soaking in SBF buffer solution for 3°days at 37°C.

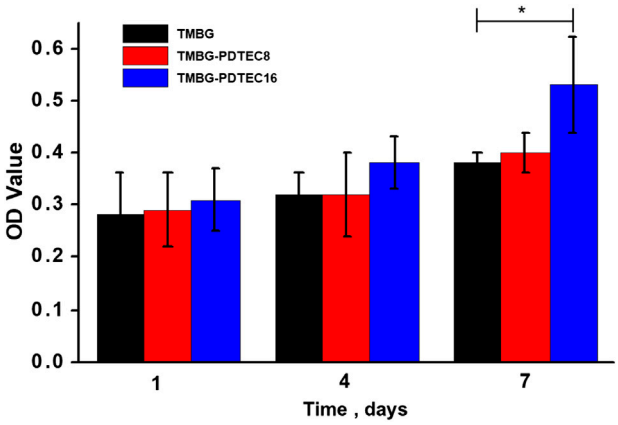

FIGURE 7 | Cell proliferation of rat bone marrow stromal cells (rBMSCs) incubated with TMBG, TMBG-PDTEC8, and TMBG-PDTEC16 scaffolds as a function of the culture period (1, 4, and 7 days). (*$p < 0.05$ compared to TMBG).

pH value of the Tris-HCl buffer solution gradually increased to 8.57 for TMBG after 28 days, and at an earlier stage, the rise in the pH value of the buffer solution was relatively faster. The increase in the pH value trend could be well balanced by introducing the PDTEC polymer into the scaffolds. **Figure 6B** indicates the weight loss profiles of the scaffolds over time. All the TMBG-PDTEC scaffolds presented a slower degradation rate than the pure TMBG, which may be associated with the formation of the coating layer, which hampered the degradation of the TMBG scaffolds. The pH auto-regulation *via* the combined decomposition of TMBG and PDTEC will be efficient to reduce the inflammation of cells/tissues surrounding the scaffold on an *in vivo* implantation (Kaushik et al., 2012).

Cell Attachment and Proliferation

In order to evaluate their biological properties, the attachment and proliferation of bone marrow stromal cells on the TMBG and TMBG-PDTEC scaffolds were assessed for culture of 1, 4, and 7 days **Figure 7** demonstrates the cell growth during the culture time for all tested conditions. The cell viability of TMBG-PDTEC16 was 1.39 times higher than TMBG after a 7-days culture, indicating that PDTEC decoration improved cell proliferation. The proliferation levels of the remaining groups were similar at all time points. Cells morphologies were further investigated by SEM observation. As shown in **Figure 8**, compared to TMBG scaffolds, bone marrow stromal cells showed better spreading on the TMBG-PDTEC scaffolds, suggesting that the TMBG-PDTEC scaffolds can enhance cell adhesion, spreading, and proliferation. The improved cyto-biocompatibility could be associated with their macro/micro/meso hierarchical bone-mimicking architecture (Li et al., 2013; Zhu et al., 2017; Li et al., 2018) as well as the facilitated biomineralization capacity (Tang et al., 2016).

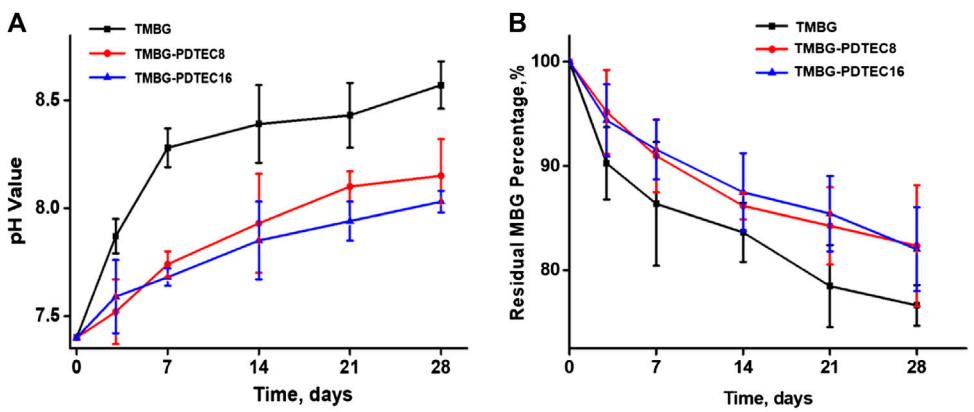

FIGURE 6 | Degradation behaviors of TMBG scaffolds: **(A)** the pH value change of Tris-HCl buffer solution incubated with scaffolds at different soaking periods; **(B)** the degradation curves of scaffolds as a function of soaking time. ($n = 3$).

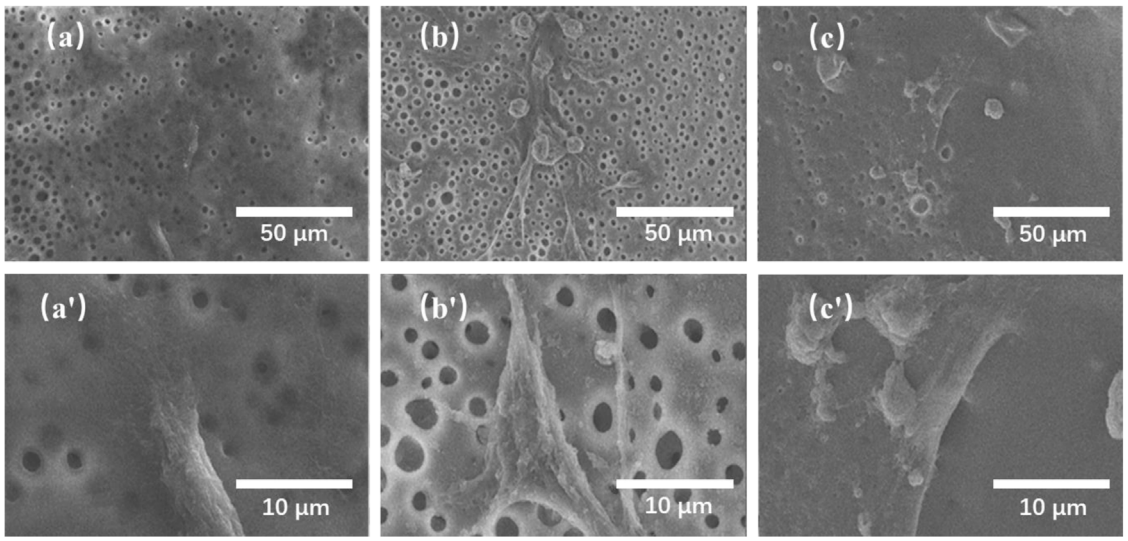

FIGURE 8 | SEM images of rat bone marrow stromal cells (rBMSCs) cultured on the TMBG **(A, A′)**, TMBG-PDTEC8 **(B, B′)**, and TMBG-PDTEC16 **(C, C′)** scaffolds for 1 day.

DISCUSSION

To obtain the hierarchical architecture, our group recently developed a kind of mesoporous bioactive glass (MBG) scaffold with trimodal macro/micro/mesoporous via a "sol-gel and polyurethane sponge templating process", where MBG sol was firstly infiltrated into the sponge, followed by sinter treatment, to produce the final TMBG scaffolds. It was found that the interconnected macroporous structure (100–500 μm) was beneficial for the promotion of nutrient exchange and waste removal processes, offer sufficient space for cell movements, proliferation, differentiation, promote bone formation and vascularization, and the ingrowth of new bone and tissue (Li et al., 2008; Zhao et al., 2015; Maria Vallet-Reg, 2016; Dashnyam et al., 2017; Gu et al., 2017; Zhu et al., 2017). It can be observed from the SEM images that we have successfully developed a scaffold with a macro/micro/mesoporous layered structure mimicking the structure of natural bone. This scaffold is beneficial to cell migration, nutrient and oxygen transport, and bone inward growth, therefore is a potential scaffold material to support bone regeneration (Yan et al., 2019).

Many studies have shown that if the scaffold degrades too quickly, it cannot create enough time for bone growth in order to complete bone repair. If the degradation is too slow and cannot provide enough space for new bone growth, materials such as calcium phosphate will cause inhibitory effects for bone regeneration (Ma et al., 2016), which is a major drawback. Subsequent researchers studied MBG coatings such as PEGylated polyglyceryl sebacate, which enhanced the strength of MBG scaffolds and could load BMP-2 factors for osteogenesis research, but the coating had some drawbacks such as uncontrollable degradation *in vivo* and other factors that need further verification in clinical practice (Chai et al., 2017; Niu et al., 2019). Our synthesized TMBG scaffolds and polymer-coated composite scaffolds show combinative priorities in mechanical robustness, and adjustable degradation rate (**Scheme 2**). Furthermore, all the components used for the construction of the scaffolds have been approved by the FDA (Tangpasuthadol et al., 2000a; Tangpasuthadol et al., 2000b). At the same time, the coating results in the slow release of material ions. Polymers at different concentrations which produce coatings with different thicknesses, result in a slower release of matrix material ions which reflect the degradation of the scaffolds. However, the degradation rate of all the current TMBG-PDTEC scaffolds was almost the same, suggesting that the thickness of the coating should be similar. The cell activity and proliferation of the subsequent materials may indirectly prove that the small molecules of the degradation products of the coating polymer are conducive to cell survival and regulation on local microenvironment adjustment, thereby facilitating certain cells to achieve *in-situ* tissue regeneration (Li et al., 2017). There are other limitations in this study including that we simply used rat-derived cells rather than used human-derived cells for cell attachment and proliferation research, which is not sufficient to prove the versatility of the scaffold in bone tissue engineering. More detailed and comprehensive studies will be performed *in vitro* and *in vivo* specifically for osteogenesis, including gene expression, protein analysis in osteogenic media, and histological studies to further demonstrate the potential for clinical applications.

Nowadays, orthopedic diseases, especially the healing of large bone defects, remain as a challenge for surgeons. The drawbacks of traditional treatments using auto-/allografting bone tissues, such as unavoidable injury, infection, disease transmission, and immune rejection, necessitate the need for artificial bone substitutes (Lin et al., 2019). MBG has been demonstrated as a potential candidate for bone replacement, which could efficiently facilitate osteogenic differentiation via its released ions (Ge et al., 2019). However, the translational application of MBG is limited by its unregular inner structure and insufficient mechanical strength (Zhang et al., 2016). In the current study, a TMBG scaffold with controllable multi-structures

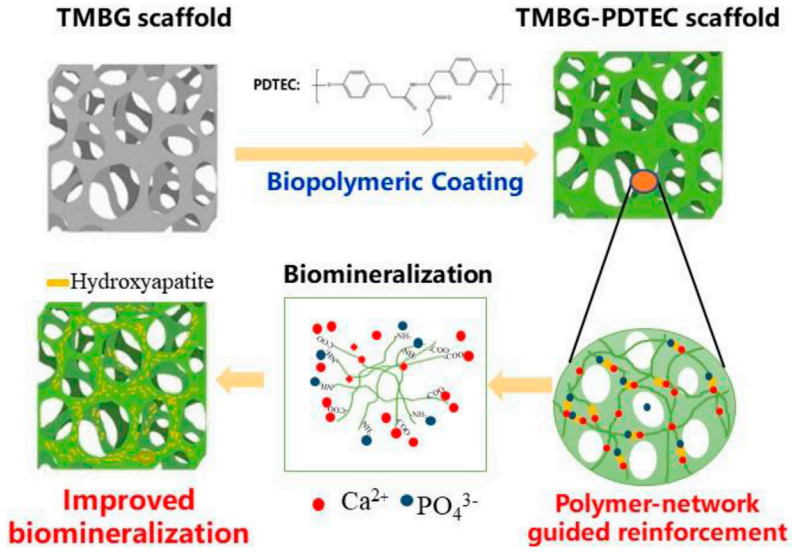

SCHEME 2 | Schematic representation of the reinforcement and biomineralization mechanisms of the TMBG-PDTEC scaffolds.

was prepared through our innovative strategy, which was expected to facilitate cell attachment/proliferation, the ingrowth of vascularized bone, and nutrient/waste exchange. More importantly, as shown in **Scheme 2**, the lack of mechanical strength was largely resolved by PDTEC adhesion, matching the load-bearing range of trabecular bone (2–12 MPa), thus ensuring that the strength of the TMBG scaffold would be sufficient as a bone substitute. Meanwhile, this polymer coating increased biomineralization, cell proliferation, and attachment/spreading, which should be beneficial for bone regeneration. Thereby, the current study provides an improved new approach to fabricate biomimicking scaffolds for the regeneration of bone.

CONCLUSION

In this study, we have demonstrated that biological active scaffolds with a macroporous/microporous/mesoporous hierarchical architecture were successfully prepared by a sol-gel and sponge-templated approach, followed by coating with tyrosine-derived polycarbonate on the scaffold surface. The resulting scaffolds not only improved the mechanical properties of the scaffolds to match the bearing range of trabecular bone (2–12 MPa), but also promoted the adhesion, spread, and proliferation of stromal cells, and significantly accelerated their biomineralization ability, thereby offering high potential for bone regeneration applications.

DATA AVAILABILITY STATEMENT

The original contributions presented in the study are included in the article/**Supplementary Material**, further inquiries can be directed to the corresponding authors.

AUTHOR CONTRIBUTIONS

RL and PX completed the experiment, and wrote and drafted this article. LX, ZI, and YL made suggestions and revised the manuscript. SZ revised part of the format of the manuscript. JK, XQ, and CL supervised and revised the manuscript. All authors contributed to this article and checked the submitted version.

FUNDING

The research was supported by the National Key R&D Program of China (2018YFE0201500 and 2017YFB0309300), the National Natural Science Foundation of China (81772317 and 51973060), the National Natural Science Foundation of China for Innovative Research Groups (51621002), and Frontiers Science Center for Materiobiology and Dynamic Chemistry. A funding grant from the Shanghai International Cooperation Program (15520721200) is also acknowledged.

ACKNOWLEDGMENTS

During the period of completing the research of this article, some of the authors were students and faculty members of the East China University of Science and Technology. Thanks to them for their help in the authors' experiment. The authors thanks Dr. Joachim Kohn for his help in material research and Dr. Lan Xiao for her help in language editing.

SUPPLEMENTARY MATERIAL

The Supplementary Material for this article can be found online at: https://www.frontiersin.org/articles/10.3389/fmats.2020.622669/full#supplementary-material.

REFERENCES

Aamer, K. A., Stafford, C. M., Richter, L. J., Kohn, J., and Becker, M. L. (2009). Thin film elastic modulus of degradable tyrosine-derived polycarbonate biomaterials and their blends. *Macromolecules* 42 (4), 1212–1218. doi:10.1021/ma802115b

Baino, F., Fiorilli, S., and Vitale-Brovarone, C. (2016). Bioactive glass-based materials with hierarchical porosity for medical applications: review of recent advances. *Acta Biomater.* 42, 18–32. doi:10.1016/j.actbio.2016.06.033

Bosetti, M. and Cannas, M. (2005). The effect of bioactive glasses on bone marrow stromal cells differentiation. *Biomaterials* 26 (18), 3873–3879. doi:10.1016/j.biomaterials.2004.09.059

Cai, L., Lin, D., Chai, Y., Yuan, Y., and Liu, C. (2018). MBG scaffolds containing chitosan microspheres for binary delivery of IL-8 and BMP-2 for bone regeneration. *J. Mater. Chem. B* 6 (27), 4453–4465. doi:10.1039/c8tb00875b

Chai, Y., Lin, D., Ma, Y., Yuan, Y., and Liu, C. (2017). RhBMP-2 loaded MBG/PEGylated poly(glycerol sebacate) composite scaffolds for rapid bone regeneration. *J. Mater. Chem. B* 5 (24), 4633–4647. doi:10.1039/C7TB00505A

Chauvel-Lebret, D. J., Pellen-Mussi, P., Auroy, P., and Bonnaure-Mallet, M. (1999). Evaluation of the *in vitro* biocompatibility of various elastomers. *Biomaterials* 20 (3), 291–299. doi:10.1016/S0142-9612(98)00181-1

Dashnyam, K., Jin, G. Z., Kim, J. H., Perez, R., Jang, J. H., and Kim, H. W. (2017). Promoting angiogenesis with mesoporous microcarriers through a synergistic action of delivered silicon ion and VEGF. *Biomaterials* 116, 145–157. doi:10.1016/j.biomaterials.2016.11.053

Du, J., Xie, P., Lin, S., Wu, Y., Zeng, D., Li, Y., et al. (2018). Time-phase sequential utilization of adipose-derived mesenchymal stem cells on mesoporous bioactive glass for restoration of critical size bone defects. *ACS Appl. Mater. Interfaces* 10 (34), 28340–28350. doi:10.1021/acsami.8b08563

Duan, B., Niu, H., Zhang, W., Ma, Y., Yuan, Y., and Liu, C. (2017). Microporous density-mediated response of MSCs on 3D trimodal macro/micro/nano-porous scaffolds via fibronectin/integrin and FAK/MAPK signaling pathways. *J. Mater. Chem. B* 5 (19), 3586–3599. doi:10.1039/C7TB00041C

Fukushima, K. (2016). Poly(trimethylene carbonate)-based polymers engineered for biodegradable functional biomaterials. *Biomater. Sci.* 4 (1), 9–24. doi:10.1039/c5bm00123d

García, A., Izquierdo-Barba, I., Colilla, M., de Laorden, C. L., and Vallet-Regí, M. (2011). Preparation of 3-D scaffolds in the SiO2-P2O5 system with tailored hierarchical meso-macroporosity. *Acta Biomater.* 7 (3), 1265–1273. doi:10.1016/j.actbio.2010.10.006

Ge, Y.-W., Lu, J.-W., Sun, Z.-Y., Liu, Z.-Q., Zhou, J., Ke, Q.-F., et al. (2019). Ursolic acid loaded-mesoporous bioglass/chitosan porous scaffolds as drug delivery system for bone regeneration. *Nanomed. Nanotechnol. Biol. Med.* 18, 336–346. doi:10.1016/j.nano.2018.10.010

Goyal, R., Vega, M. E., Pastino, A. K., Singh, S., Guvendiren, M., Kohn, J., et al. (2017). Development of hybrid scaffolds with natural extracellular matrix deposited within synthetic polymeric fibers. *J. Biomed. Mater. Res.* 105 (8), 2162–2170. doi:10.1002/jbm.a.36078

Gu, Z., Wang, S., Weng, W., Chen, X., Cao, L., Wei, J., et al. (2017). Influences of doping mesoporous magnesium silicate on water absorption, drug release, degradability, apatite-mineralization and primary cells responses to calcium sulfate based bone cements. *Mater. Sci. Eng. C Mater. Biol. Appl.* 75, 620–628. doi:10.1016/j.msec.2017.02.100

Kaushik, C., Kraigsley, A. M., and Durgadas, B. (2012). Gas-foamed scaffold gradients for combinatorial screening in 3D. *J. Funct. Biomater.* 3 (1), 173–182. doi:10.3390/jfb3010173

Kim, J., Dadsetan, M., Ameenuddin, S., Windebank, A. J., Yaszemski, M. J., and Lu, L. (2010). *In vivo* biodegradation and biocompatibility of PEG/sebacic acid-based hydrogels using a cage implant system. *J. Biomed. Mater. Res.* 95 (1), 191–197. doi:10.1002/jbm.a.32810

Li, J., Jiang, F., Yang, B., Song, X. R., Liu, Y., Yang, H. H., et al. (2013). Topological insulator bismuth selenide as a theranostic platform for simultaneous cancer imaging and therapy. *Sci. Rep.* 3, 1998. doi:10.1038/srep01998

Li, Q., Lin, H., Du, Q., Liu, K., Wang, O., Evans, C., et al. (2018). Scalable and physiologically relevant microenvironments for human pluripotent stem cell expansion and differentiation. *Biofabrication* 10 (2), 025006. doi:10.1088/1758-5090/aaa6b5

Li, X., Xie, J., Yuan, X., and Xia, Y. (2008). Coating electrospun poly(epsilon-caprolactone) fibers with gelatin and calcium phosphate and their use as biomimetic scaffolds for bone tissue engineering. *Langmuir* 24 (24), 14145–14150. doi:10.1021/la802984a

Li, Y., Xiao, Y., and Liu, C. (2017). The horizon of Materiobiology: a perspective on material-guided cell behaviors and tissue engineering. *Chem. Rev.* 117 (5), 4376–4421. doi:10.1021/acs.chemrev.6b00654

Lin, D., Chai, Y., Ma, Y., Duan, B., Yuan, Y., and Liu, C. (2019). Rapid initiation of guided bone regeneration driven by spatiotemporal delivery of IL-8 and BMP-2 from hierarchical MBG-based scaffold. *Biomaterials* 196, 122–137. doi:10.1016/j.biomaterials.2017.11.011

Lin, D., Yang, K., Tang, W., Liu, Y., Yuan, Y., and Liu, C. (2015). A poly(glycerol sebacate)-coated mesoporous bioactive glass scaffold with adjustable mechanical strength, degradation rate, controlled-release and cell behavior for bone tissue engineering. *Colloids Surf. B Biointerfaces* 131, 1–11. doi:10.1016/j.colsurfb.2015.04.031

Ma, Y., Zhang, W., Wang, Z., Wang, Z., Xie, Q., Niu, H., et al. (2016). PEGylated poly(glycerol sebacate)-modified calcium phosphate scaffolds with desirable mechanical behavior and enhanced osteogenic capacity. *Acta Biomater.* 44, 110–124. doi:10.1016/j.actbio.2016.08.023

Marelli, B., Ghezzi, C. E., Mohn, D., Stark, W. J., Barralet, J. E., Boccaccini, A. R., et al. (2011). Accelerated mineralization of dense collagen-nano bioactive glass hybrid gels increases scaffold stiffness and regulates osteoblastic function. *Biomaterials* 32 (34), 8915–8926. doi:10.1016/j.biomaterials.2011.08.016

Niu, H., Ma, Y., Wu, G., Duan, B., Wang, Y., Yuan, Y., et al. (2021). Corrigendum to "Multicellularity-interweaved bone regeneration of BMP-2-loaded scaffold with orchestrated kinetics of resorption and osteogenesis"[Biomaterials Volume 216 (2019) 119216]. *Biomaterials* 264, 120376. doi:10.1016/j.biomaterials.2020.120376

Pei, P., Qi, X., Du, X., Zhu, M., Zhao, S., and Zhu, Y. (2016). Three-dimensional printing of tricalcium silicate/mesoporous bioactive glass cement scaffolds for bone regeneration. *J. Mater. Chem. B* 4 (46), 7452–7463. doi:10.1039/C6TB02055K

Schumacher, M., Reither, L., Thomas, J., Kampschulte, M., Gbureck, U., Lode, A., et al. (2017). Calcium phosphate bone cement/mesoporous bioactive glass composites for controlled growth factor delivery. *Biomater. Sci.* 5 (3), 578–588. doi:10.1039/c6bm00903d

Souza, M. T., Tansaz, S., Zanotto, E. D., and Boccaccini, A. R. (2017). Bioactive glass fiber-reinforced PGS matrix composites for cartilage regeneration. *Materials* 10 (1), 83. doi:10.3390/ma10010083

Tang, W., Lin, D., Yu, Y., Niu, H., Guo, H., Yuan, Y., et al. (2016). Bioinspired trimodal macro/micro/nano-porous scaffolds loading rhBMP-2 for complete regeneration of critical size bone defect. *Acta Biomater.* 32, 309–323. doi:10.1016/j.actbio.2015.12.006

Tang, W., Yuan, Y., Lin, D., Niu, H., and Liu, C. (2014). Kaolin-reinforced 3D MBG scaffolds with hierarchical architecture and robust mechanical strength for bone tissue engineering. *J. Mater. Chem. B* 2 (24), 3782–3790. doi:10.1039/c4tb00025k

Tangpasuthadol, V., Pendharkar, S. M., and Kohn, J. (2000a). Hydrolytic degradation of tyrosine-derived polycarbonates, a class of new biomaterials. Part I: study of model compounds. *Biomaterials* 21 (23), 2371–2378. doi:10.1016/S0142-9612(00)00104-6

Tangpasuthadol, V., Pendharkar, S. M., Peterson, R. C., and Kohn, J. (2000b). Hydrolytic degradation of tyrosine-derived polycarbonates, a class of new biomaterials. Part II: 3-yr study of polymeric devices. *Biomaterials* 21 (23), 2379–2387. doi:10.1016/S0142-9612(00)00105-8

Vallet-Reg, M., Antonio, J., and Salinas, A. D. A. (2016). Tailoring the structure of bioactive glasses: from the nanoscale to macroporous scaffolds. *Int. J. Appl. Glass Sci.* 7 (2), 195–205. doi:10.1111/ijag.12205

Wu, C., Miron, R., Sculean, A., Kaskel, S., Doert, T., Schulze, R., et al. (2011). Proliferation, differentiation and gene expression of osteoblasts in boron-containing associated with dexamethasone deliver from mesoporous bioactive glass scaffolds. *Biomaterials* 32 (29), 7068–7078. doi:10.1016/j.biomaterials.2011.06.009

Wu, C., Zhang, Y., Zhu, Y., Friis, T., and Xiao, Y. (2010). Structure-property relationships of silk-modified mesoporous bioglass scaffolds. *Biomaterials* 31 (13), 3429–3438. doi:10.1016/j.biomaterials.2010.01.061

Wu, C., Zhou, Y., Xu, M., Han, P., Chen, L., Chang, J., et al. (2013). Copper-containing mesoporous bioactive glass scaffolds with multifunctional properties of angiogenesis capacity, osteostimulation and antibacterial activity. *Biomaterials* 34 (2), 422–433. doi:10.1016/j.biomaterials.2012.09.066

Xie, P., Du, J., Li, Y., Wu, J., He, H., Jiang, X., et al. (2019). Robust hierarchical porous MBG scaffolds with promoted biomineralization ability. *Colloids Surf. B Biointerfaces* 178, 22–31. doi:10.1016/j.colsurfb.2019.02.042

Yan, Y., Chen, H., Zhang, H., Guo, C., Yang, K., Chen, K., et al. (2019). Vascularized 3D printed scaffolds for promoting bone regeneration. *Biomaterials* 190–191, 97–110. doi:10.1016/j.biomaterials.2018.10.033

Yang, K., Zhang, J., Ma, X., Ma, Y., Kan, C., Ma, H., et al. (2015). β-Tricalcium phosphate/poly(glycerol sebacate) scaffolds with robust mechanical property for bone tissue engineering. *Mater. Sci. Eng. C Mater. Biol. Appl.* 56, 37–47. doi:10.1016/j.msec.2015.05.083

Yu, C. and Kohn, J. (1999). Tyrosine-PEG-derived poly(ether carbonate)s as new biomaterials. Part I: synthesis and evaluation. *Biomaterials* 20 (3), 253–264. doi:10.1016/S0142-9612(98)00169-0

Zeng, D., Zhang, X., Wang, X., Huang, Q., Wen, J., Miao, X., et al. (2017). The osteoimmunomodulatory properties of MBG scaffold coated with amino functional groups. *Artif Cells Nanomed Biotechnol* 46 (7), 1–11. doi:10.1080/21691401.2017.1369428

Zhang, X., Zeng, D., Li, N., Wen, J., Jiang, X., Liu, C., et al. (2016). Functionalized mesoporous bioactive glass scaffolds for enhanced bone tissue regeneration. *Sci. Rep.* 6, 19361. doi:10.1038/srep19361

Zhao, S., Zhang, J., Zhu, M., Zhang, Y., Liu, Z., Ma, Y., et al. (2015). Effects of functional groups on the structure, physicochemical and biological properties of mesoporous bioactive glass scaffolds. *J. Mater. Chem. B* 3 (8), 1612–1623. doi:10.1039/c4tb01287a

Zhou, P., Xia, Y., Jiang, L., Zhang, Y., Qiu, C., Xie, Y., et al. (2016). O-Acrylamidomethyl-2-hydroxypropyltrimethyl ammonium chloride chitosan and silk modified mesoporous bioactive glass scaffolds with excellent mechanical properties, bioactivity and long-lasting antibacterial activity. *RSC Adv.* 6 (71), 66938–66948. doi:10.1039/C6RA11463F

Zhou, Y., Shi, M., Jones, J. R., Chen, Z., Chang, J., Wu, C., et al. (2017). Strategies to direct vascularisation using mesoporous bioactive glass-based biomaterials for bone regeneration. *Int. Mater. Rev.* 62 (7), 392–414. doi:10.1080/09506608.2016.1266744

Zhu, C., Pongkitwitoon, S., Qiu, J., Thomopoulos, S., and Xia, Y. (2018). Design and fabrication of a hierarchically structured scaffold for tendon-to-bone repair. *Adv. Mater.* 30 (16), 1707306. doi:10.1002/adma.201707306

Zhu, Y., Zhang, K., Zhao, R., Ye, X., Chen, X., Xiao, Z., et al. (2017). Bone regeneration with micro/nano hybrid-structured biphasic calcium phosphate bioceramics at segmental bone defect and the induced immunoregulation of MSCs. *Biomaterials* 147, 133–144. doi:10.1016/j.biomaterials.2017.09.018

Conflict of Interest: The authors declare that the research was conducted in the absence of any commercial or financial relationships that could be construed as a potential conflict of interest.